Report of the Annual Meeting

Numerical Results of the Complex Gross-Pitaevskii Equation

匡昱潼

mentor：蔡勇勇

School of Mathematical Science

Computational Mathematics

December 22, 2023

Background

- Bose-Einstein Condensation (BEC) was predicted by Bose and Einstein in 1924-1925. The condensate was obtained experimentally for the first time in 1995 in a system consisting of about half a million alkali atoms cooled down to nanokelvin-level temperatures.

Background

- Bose-Einstein Condensation (BEC) was predicted by Bose and Einstein in 1924-1925. The condensate was obtained experimentally for the first time in 1995 in a system consisting of about half a million alkali atoms cooled down to nanokelvin-level temperatures.
- Achieving Bose-Einstein Condensation (BEC) in atomic systems requires extremely low temperatures. This challenge has prompted exploration into realizing BEC in atomless systems at relatively higher temperatures.

Background

One possible candidate is a system of exciton-polaritons. Various mathematical models have been proposed for this new condensate. One of them, called complex GP equation, is explored there:

$$
\begin{aligned}
&i\psi_t = -\Delta\psi + V(x)\psi + |\psi|^2\psi + i\left[\omega(x) - \sigma|\psi|^2\right]\psi,\ t>0,\ x \in D = \mathbb{R}^2,\\
&\psi(x,0) = \psi_0(x), x \in D.
\end{aligned}
\tag{1}
$$

Here,$\psi = \psi(x,t)$ is the wave function of the condensate, $V(x)$ is the trapping potential, $\omega = \omega(x) \geq 0$ is the pumping terms,$\sigma > 0$ is the decaying terms.

Stationary radial solutions

We first explore the stationary solutions. Inserting $\psi(x,t) = \exp(-i\mu t)\phi(x)$ into equation (1) leads to the following equation for ϕ:

$$\mu\phi(x) = \left[-\Delta + V(x) + |\phi(x)|^2 + i\left(\omega(x) - \sigma|\phi(x)|^2\right)\right]\phi(x). \qquad (2)$$

To make μ to be real, it must be required that:

$$\int_D \left(\omega(x) - \sigma|\phi(x)|^2\right)|\phi(x)|^2 dx = 0.$$

We assume
$V(x) = |x|^2$,$\omega(x) = \alpha\Theta(R - |x|), \Theta(x) = (1 + \tanh(\kappa x))/2.$

Stationary radial solutions

Now we solve the stationary radial solution of equation (2)(i.e.$r = |x| \geq 0$). After some computation,we get the following equation:

$$\begin{aligned}
&\phi' = \varphi, \\
&\varphi' = -\frac{1}{r}\varphi - \mu\phi + r^2\phi + |\phi|^2\phi + i\left(\alpha\Theta_R - \sigma|\phi|^2\right)\phi, \\
&\xi' = \left(\alpha\Theta_R - \sigma|\phi(r)|^2\right)|\phi(r)|^2 r, \\
&\mu' = 0,
\end{aligned} \tag{3}$$

$$\phi(b) = 0, \quad \varphi(0) = 0, \quad \mathrm{Im}(\phi(0)) = 0, \quad \xi(b) = 0.$$

Stationary radial solutions

We solve system (3) with high accuracy by using a collocation method. The MATLAB function $bvp5c$ is used:

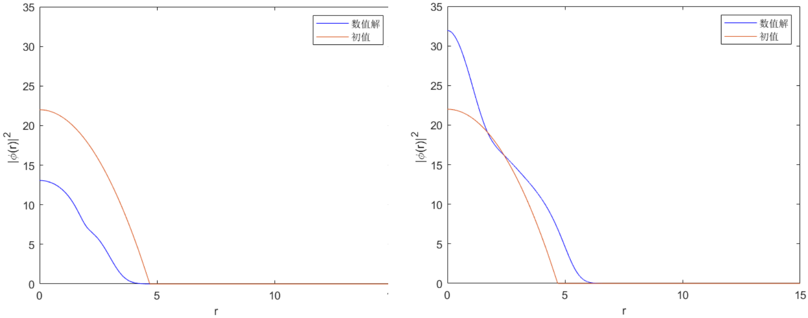

(a) R=2 **(b)** R=8

Figure 1: numerical solution of collocation method

Numerical continuation

Let us rewrite system (3) as

$$F(u, \lambda) = 0, \tag{4}$$

where $u \in \mathbb{B}$($\mathbb{B}$ is a real Banach space) is the solution of the system, λ is a real parameter(λ can be α, σ, or R).
The idea in this section is to study the dependence of the solution, $u(\lambda)$, on the parameter, λ,i.e., to trace the solution branches $[u(\lambda), \lambda]$ of (4).

Numerical continuation

Suppose that (u_0, λ_0) is a solution of the discretized problem (4) and that the directional derivative $\dot{u}_0 = du_0/d\lambda$ is known. Then the solution u_1 at $\lambda_1 = \lambda_0 + \triangle\lambda$ can be computed as

$$
\begin{cases}
F_u(u_1^i \ \lambda_1)\triangle u_1^i = -F(u_1^i, \lambda_1), \\
u_1^{i+1} = u_1^i + \triangle u_1^i, \quad i = 0, 1, 2, \cdots .
\end{cases}
$$

with

$$
u_1^0 = u_0 + \triangle\lambda\dot{u}_0,
$$

where $F_u(u, \lambda)$ is the Jacobian matrix. After convergence find $\dot{u}_1$ from

$$
F_u(u_1, \lambda_1)\dot{u}_1 = -F_\lambda(u_1, \lambda_1).
$$

Numerical continuation

To avoid folds, we can introduce a pseudo-arclength continuation method. This leads to the augmented system

$$\begin{cases} F(u(v), \lambda(v)) = 0, \\ N(u(v), \lambda(v), v) = 0. \end{cases}$$

One of the most frequently used definitions of N is:

$$N(u, \lambda, v) \equiv \dot{u}_0^T (u - u_0) + \dot{\lambda}_0 (\lambda - \lambda_0) - v.$$

Numerical continuation

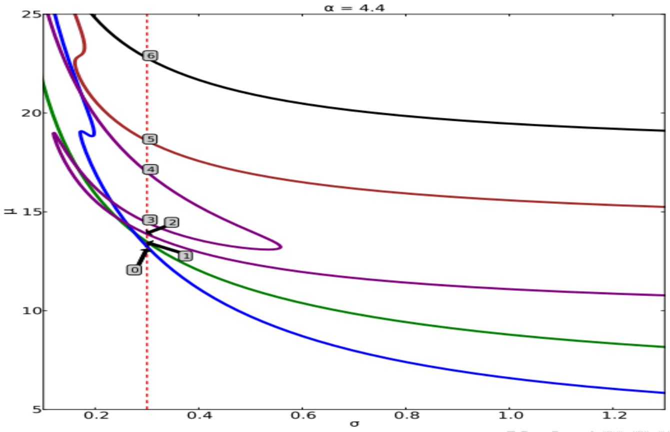

Figure 2: The chemical μ of the system (3) for different values of σ with $\alpha = 4.4$ and $R = 2$ fixed

Linear stability analysis

Consider the linear stability of the radially symmetric solutions $\psi(r,t)=\exp(-i\mu t)\phi(r)$ under the small perturbations:

$$\psi(r,\theta,t)=\exp(-i\mu t)[\phi(r)+\varepsilon(u(r)\exp(-i(m\theta+\omega t)) \\ +v^*(r)\exp(i(m\theta+\omega^* t)))],$$

with $\varepsilon << 1, m=1,2,3,\cdots$ The radially symmetric solutions are linearly unstable if $\mathrm{Im}(\omega)>0$.
The results in literature shows that,the solutions will be unstable when $R \gtrsim 4.4$ or $R \lesssim 0.6$(the specific situation is related to m).

Strange-splitting Fourier spectral method

We now investigate the dynamics of equation (1) by Strange-splitting Fourier spectral method. The situation of one dimension can be stated as:

$$
\begin{gathered}
i\psi_t = -\psi_{xx} + V(x)\psi + |\psi|^2\psi + i\left(\alpha\Theta_R - \sigma|\psi|^2\right)\psi, \\
\psi(x,0) = \psi_0(x), \quad a \le x \le b, \\
\psi(a,t) = \psi(b,t), \quad \psi_x(a,t) = \psi_x(b,t), \quad t > 0.
\end{gathered}
\tag{5}
$$

Consider $h = \Delta x = (b-a)/M > 0$ as the mesh size, where M is an even positive integer and $\tau = \Delta t > 0$ as the time step. Define Ψ_j^n as the numerical approximation of $\psi(x_j, t_n)$.

Strange-splitting Fourier spectral method

We now separate equation (5) into:

$$i\psi_t = V(x)\psi + |\psi|^2\psi + i\left(\alpha\Theta_R - \sigma|\psi|^2\right)\psi, \tag{6}$$

$$i\psi_t = -\psi_{xx}. \tag{7}$$

We combine equation (6) and (7) to approximate the solution of (5) on $[t_n, t_{n+1}]$.
Equation (6) can be solved directly, and the solution of equation (7) can be represented as $\psi(x,t) = e^{it\Delta}\psi_0$.

Strange-splitting Fourier spectral method

- Step1: From t_n to $t_n + \tau/2$, solve equation (6):

$$\Psi_j^{(1)} = \begin{cases} \Psi_j^n U_j^{(1)} e^{i\theta_j^{(1)}}, & \Theta_j > 0, \\ \Psi_j^n W_j^{(1)} e^{i\phi_j^{(1)}}, & \Theta_j = 0. \end{cases}$$

Strange-splitting Fourier spectral method

- Step1: From t_n to $t_n+\tau/2$, solve equation (6):

$$\Psi_j^{(1)} = \begin{cases} \Psi_j^n U_j^{(1)} e^{i\theta_j^{(1)}}, & \Theta_j > 0, \\ \Psi_j^n W_j^{(1)} e^{i\phi_j^{(1)}}, & \Theta_j = 0. \end{cases}$$

- Step2: From t_n to $t_n+\tau$ solve equation (7), and use $\Psi_j^{(1)}$ as initial condition:

$$\Psi_j^{(2)} = \frac{1}{M}\sum_{l=-M/2}^{M/2-1} e^{-i\omega_l^2\tau}\widehat{\Psi}_l^{(1)} e^{i\omega_l(x_j-a)}, \quad j=0,1,2,\ldots,M-1,$$

where,

$$\widehat{\Psi}_l^{(1)} = \sum_{j=0}^{M-1}\Psi_j^{(1)} e^{-i\omega_l(x_j-a)}, \quad \omega_l = \frac{2\pi l}{b-a}, \quad l=-\frac{M}{2},\ldots,\frac{M}{2}-1.$$

Strange-splitting Fourier spectral method

- Step3: From $t_n + \tau/2$ to $t_n + \tau$ solve equation (6), and use $\Psi_j^{(2)}$ as initial condition to get Ψ^{n+1}.

Numerical results

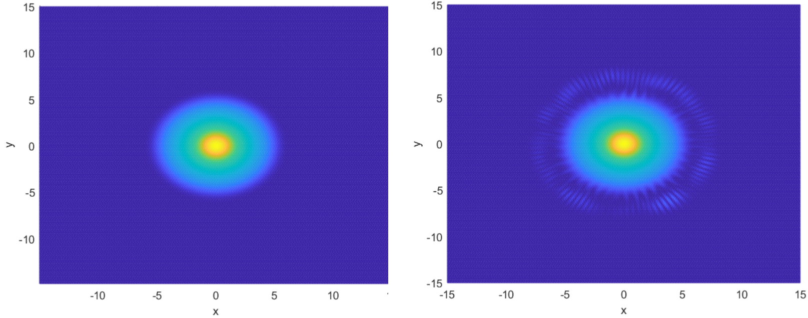

(a) t=0 **(b)** t=3

Figure 3: Simulation results for $R = 8$.The plots show the density distribution at different times. The dark blue areas represent regions where the density becomes zero.

Numerical results

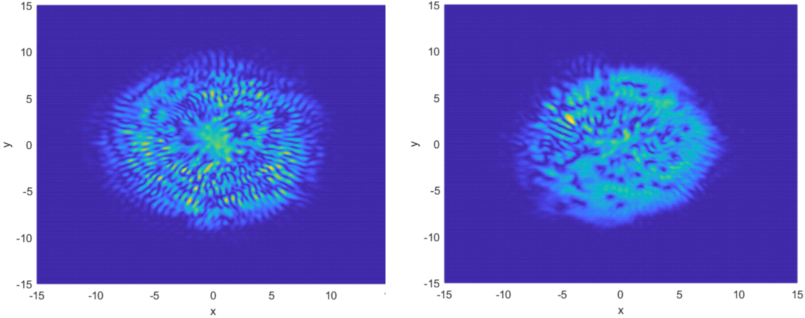

(a) t=5 **(b)** t=6

Figure 4: Simulation results for $R = 8$.The plots show the density distribution at different times. The dark blue areas represent regions where the density becomes zero.

Numerical results

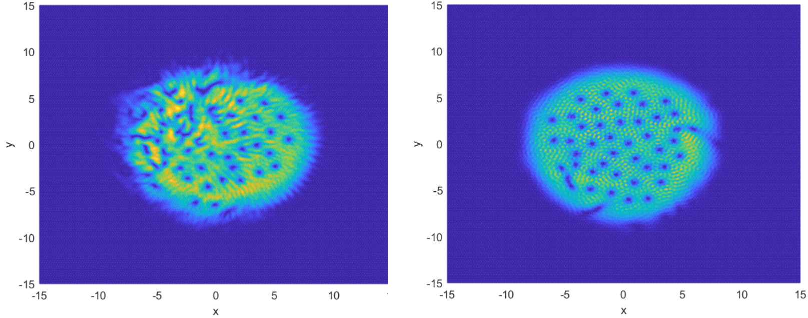

(a) t=7 **(b)** t=8

Figure 5: Simulation results for $R = 8$.The plots show the density distribution at different times. The dark blue areas represent regions where the density becomes zero.

Numerical results

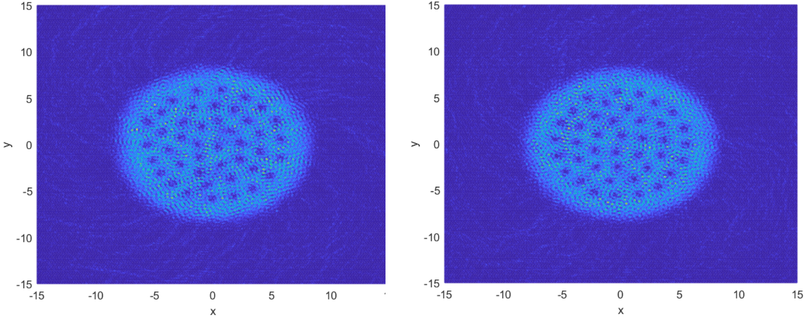

(a) t=10 **(b)** t=40

Figure 6: Simulation results for $R = 8$.The plots show the density distribution at different times. The dark blue areas represent regions where the density becomes zero.

Thanks!